Spin-wave modes in granular superferromagnetic $(SiO_2)Co/GaAs$ films observed using Brillouin light scattering

A. A. Stashkevich,[1,*] Y. Roussigné,[1] A. I. Stognij,[2] N. N. Novitskii,[2] M. P. Kostylev,[3] G. A. Wurtz,[4] A. V. Zayats,[4] and L. Lutsev[5]

[1]*LPMTM CNRS (UPR 9001), Université Paris 13, 93430 Villetaneuse, France*

[2]*Institute of Solid State and Semiconductor Physics, National Academy of Sciences of Belarus, 220072 Minsk, Belarus*

[3]*School of Physics–M013, University of Western Australia, 35 Stirling Highway, Crawley, Western Australia 6009, Australia*

[4]*Centre for Nanostructured Media, IRCEP, The Queen's University of Belfast, Belfast BT7 1NN, United Kingdom*

[5]*Research Institute "Ferrite-Domen", 196084 Saint-Petersburg, Russia*

(Received 11 April 2008; revised manuscript received 10 September 2008; published 9 December 2008)

Behavior of dipole-exchange spin waves (SWs) in the Damon-Eshbach geometry in a nanocomposite $(SiO_2)_{100-x}Co_x$ superferromagnetic ($x=80$ at. %) film has been studied by Brillouin light scattering. The measured value of the effective exchange constant turned out to be three times less than its value for the bulk cobalt. A qualitative theoretical model has been proposed to explain this reduction. It has been shown that the "superspin" approximation, identifying each nanoparticle with a "magnetic point" with no internal structure, is not sufficient to account for the description of the SW behavior of a concentrated nanocomposite medium.

DOI: 10.1103/PhysRevB.78.212404 PACS number(s): 75.30.Ds, 75.50.−y, 78.35.+c

Magnetic and electrical properties of granular films, consisting of magnetic nanoparticles in an insulating matrix, can be varied over a very wide range by independently modifying the particle sizes, their separation, and composition.[1] This explains numerous publications dedicated to both technological and academic research.[2–4]

Static as well as dynamic behavior of such systems is dominated by a trade-off between the long-range dipole-dipole interaction (DDI) and short-range exchange coupling between individual nanoelements, also known as *superspins* in the case of small single-domain nanoparticles. The major static features of highly diluted assemblies, i.e., those of isolated magnetic nanoparticles in the absence of interparticle interactions, are well described by the model of Brown,[5] which provides a relatively simple and clear physical picture. The behavior of isolated particles, determined in this approximation by the thermally activated relaxation between the potential wells of the anisotropy energy, is well verified by the magnetization and low-frequency susceptibility measurements in a wide temperature range for the samples "prepared" according to different scenarios.[6]

Introduction of DDIs, however weak, leads to serious theoretical complications due to their long-range nature.[7] Numerous papers have been dedicated to the investigations of the influence of DDIs on the static behavior and low-frequency dynamics of assemblies of interacting magnetic dipoles well under the percolation threshold.[8,9]

However, the physical picture of collective magnetic behavior is incomplete without taking into account the exchange interaction. In this respect, much original research has been done on a particular variety of dense nanocomposite materials known as discontinuous metal-insulator multilayers (DMIMs) comprised of CoFe nanoparticles in an Al_2O_3 matrix.[10,11] Such relatively dense multilayers have demonstrated the full spectrum of possible types of behaviors. The transition from superparamagnetism (SPM) (Ref. 10) to superferromagnetism (SFM) (Ref. 11) via the superspin-glass (SSG) (Ref. 10) state has been implemented by simply varying the particle diameter–to–interlayer distance ratio.

Another group of papers, falling into in a far less numerous category, has been dedicated to fast dynamics, more precisely to microwave properties of saturated magnetic nanogranular materials in the gigahertz range.[12,13] The investigations of the ferromagnetic resonance (FMR) in magnetically heterogeneous Fe-SiO_2 composite thin films in the vicinity of the percolation threshold have demonstrated the presence of spin-wave resonances (SWRs). However, the effective exchange constant was very small.

The FMR technique, based on the resonant amplification of the exciting high-frequency electromagnetic field, is extremely sensitive. However, FMR characterization of collective magnetic excitations is incomplete, being limited to spatially uniform external microwave pumping. In contrast, Brillouin light-scattering (BLS) spectroscopy can access the SW excitations with the wave numbers in the extremely wide range of 3×10^3 cm$^{-1}<k<2\times10^5$ cm^{-1}, which allows tracing the full SW dispersion curve even in relatively thin samples.

The specificity of the case addressed in this Brief Report lies in the fact that a monolayer structure is comprised of spherical nanoelements whose size is much less than the SW wavelength ($\lambda_{sw}>250$ nm). At the same time, the size of nanograins in composite materials investigated in this paper is on the order of 5 nm, which ensures the collective character of the microwave dynamics of the system. In the present Brief Report, the influence of the interparticle exchange interaction on the spectra of thermal magnons propagating in thin nanogranular films will be studied. To this end, dispersion characteristics of such dipole-exchange SW, measured by the BLS technique, will be analyzed, aided by numerical simulations.

The experiments were performed on samples of amorphous silicon dioxide films containing cobalt nanoparticles grown on a gallium arsenide substrate.[14] *n*-GaAs substrates are of the (100)-orientation type. The GaAs substrate thickness is 0.4 mm.

 ©2008 The American Physical Society

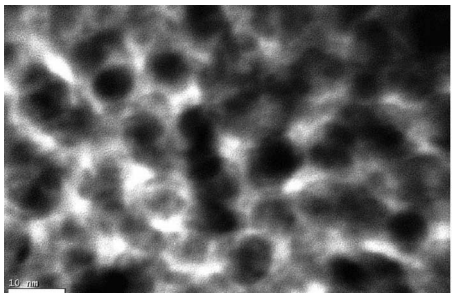

FIG. 1. High-resolution TEM image of the sample.

The SiO_2(Co) films were grown on GaAs substrates by ion-beam cosputtering of composite quartz and cobalt targets. The concentration of cobalt nanoparticles in the silicon dioxide deposit was varied by changing the ratio of cobalt and quartz target areas. For BLS experiments we have selected a 120-nm-thick SiO_2(Co) film ($h=120$ nm) with atomic concentration $x=80\%$. The latter corresponds to subnanometer interparticle spacing d assessed from x via the calculation of the volume concentration of Co. The film composition was determined by x-ray analysis. It has been double-checked by Rutherford backscattering.

To estimate the actual size of the particles, we have employed two independent techniques: low-angle x-ray scattering and transmission electron microscope (TEM) imaging. Using an FEI FIB200TEM nanomachining system, a parallel-sided lamella (~300 nm) was milled to prepare the cross-sectional cut. The cross section was imaged with a JEOL 2010 (200 kV) TEM. According to the low-angle x-ray-scattering measurements, the average size of cobalt particles is on the order of 3–4 nm. However, the values retrieved from high-resolution TEM images (see Fig. 1) are slightly greater, being on the order of 5–6 nm.

The BLS measurements (p-s scattering) were carried out in the Damon-Eshbach (DE) geometry. The saturating magnetic $\vec{H}$ field was applied parallel to the plane of the film and the direction of propagation of a SW was normal to $\vec{H}$. Light from a single-mode Ar^+ laser using a power of 350 mW at wavelength λ of 514 nm was focused onto the sample and the frequency spectrum of the backscattered light was analyzed using a computer-controlled Sandercock-type (2×3)-pass tandem Fabry-Pérot interferometer. The value of the wave number k was changed by varying the angle of incident light θ measured against the surface normal to the sample.

The results obtained are presented in Figs. 2 and 3. In Fig. 2 are plotted Stokes and anti-Stokes frequency shifts as functions of the angle of incidence with (a) $H=3000$ Oe and (b) $H=5000$ Oe in comparison with theoretical curves. In our calculations we used the magnetic Green's-function formalism in the nondiagonal approximation.[15] The order of the matrix reduction was set equal to 5, which allowed us to trace dispersion curves for the DE or magnetostatic surface wave (MSSW), as well as the dispersion of the first four backward volume spin waves (BVSWs) which lie within the DE waveband. We assumed the presence of the uniaxial anisotropy with its axis perpendicular to the composite film plane. We have set the effective exchange constant as A_{eff}

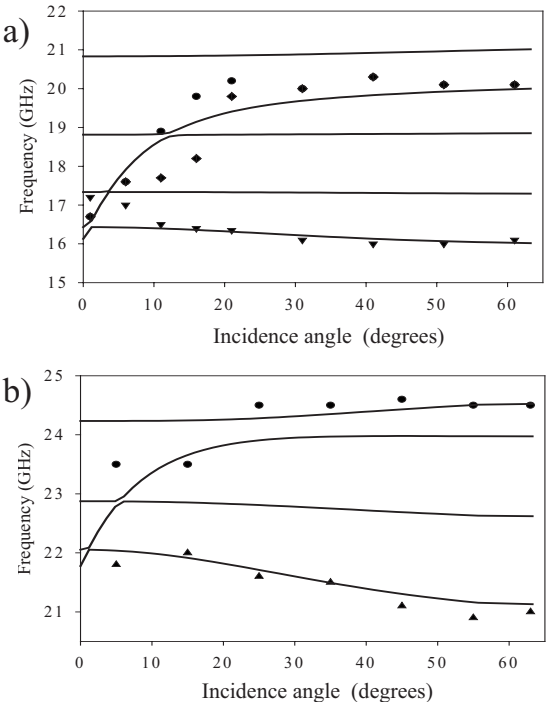

FIG. 2. Spin-wave frequencies vs angle of incidence: (a) $H=3000$ Oe and (b) $H=5000$ Oe.

$=0.5\times10^{-6}$ erg cm^{-1}, i.e., equal to its best-fit value obtained from numerical simulations of the fine structure of BLS lines (see Fig. 3). The best fit corresponds to $H_a=800$ Oe ($H=5000$ Oe) and $H_a=320$ Oe ($H=3000$ Oe), while the saturation magnetization in both cases was taken equal to $4\pi M_s=8700$ G. Magnetic anisotropy influences mainly the lowest bulk mode, whose contribution to BLS is the most significant. Higher modes, pushed upward by the exchange, behave themselves as spin-wave resonances with very little dispersion. It is hybridization with the DE mode and subsequent repulsion of interacting branches that make them slightly dispersive [e.g., see the highest mode in Fig. 2(b)]. The origin of this anisotropy is not of crystalline nature: the Co nanospheres have cubic structure, although slight traces of the hexagonal phase are visible in x-ray measurements. This means that it is due to macroscopic factors such as partial ordering during the film deposition or a deviation from the spherical shape of the particles. It should be noted that pronounced magnetic anisotropy has already been reported in Co-Al_2O_3 nanocomposite structures.[13]

To maximize the frequency bandwidth, which is instrumental for revealing SW dispersion, we used relatively low values of magnetic fields and the sample was not fully saturated. This means, in particular, that the effective value of their intrinsic parameters could vary, including the saturation magnetization and magnetic anisotropy. The experimental data in Fig. 2 were retrieved from theoretical analysis of the fine structure of the BLS spectra which are discussed in detail below.

We quantified the value of the exchange constant A by comparing the measured and the theoretical shapes of the Stokes and anti-Stokes BLS lines. For our computer simulations, considering the thermal stochastic nature of the mag-

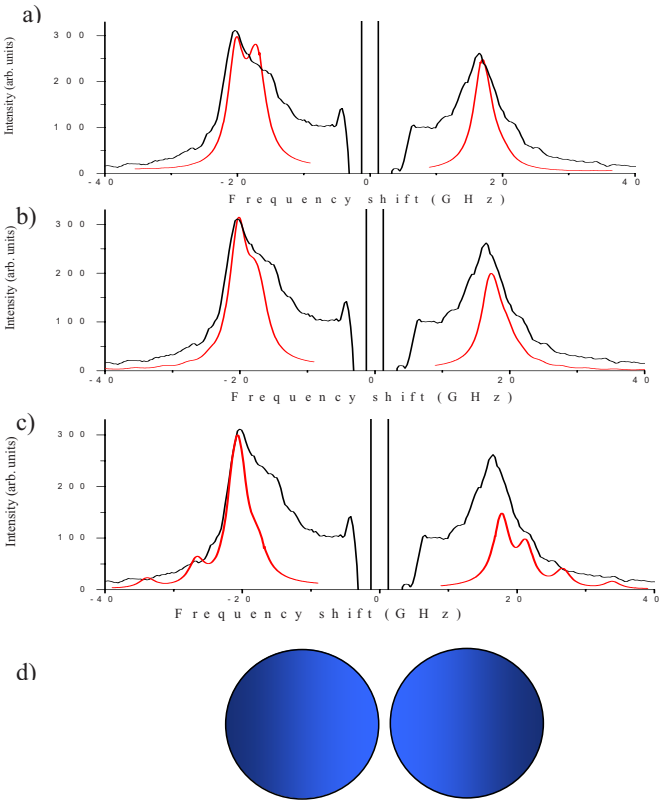

FIG. 3. (Color online) Results of computer simulations of the fine structure of a BLS spectral line for three fitting values of the effective exchange constant for $H=3000$ Oe: (a) $A_{\text{eff}}=0.2\times10^{-6}$ erg cm^{-1}, (b) $A_{\text{eff}}=0.5\times10^{-6}$ erg cm^{-1}, and (c) $A_{\text{eff}}=1.8\times10^{-6}$ erg cm^{-1} (bulk cobalt value). A second curve in each figure represents the experimental results for the case considered. (d) Geometry of interparticle exchange interaction.

nons, we employed the code based on the fluctuation-dissipation theorem (FDT) and optical Green's functions for a multilayer, described in more detail in Ref. 16.

Figure 3 presents the results of computer simulations of the fine structure of a BLS spectral line. As can be seen, the experimental anti-Stokes line, in the case $\theta=20°$ and $H=3000$ Oe, has a very characteristic shape. Major features of its shape are explained by the following considerations. As in the usual continuous ferromagnetic films, there are two contributions to the BLS spectrum: that of the DE modes and the collective contribution of BVSWs. In our relatively thick sample the latter can superimpose and form a wide peak of a characteristic shape. The Stokes and anti-Stokes responses from BVSWs are symmetric, while the DE mode produces a distinctly asymmetric Stokes and anti-Stokes pattern. Thus the BLS spectra are marked by a clearly observable asymmetry of Stokes and anti-Stokes lines which rapidly increases with the growth of the angle of incidence. In other words, basically, for $\theta=20°$, the Stokes response is dominated by the DE contribution, while the anti-Stokes one is dominated by the SWRs. The frequency positions of these peaks are marked with squares and triangles, respectively, while theoretical results are represented by a solid line. Circles appearing in Fig. 2(b) correspond to the presence of a fine structure in the anti-Stokes line, which implies reliable identification of the extremity of the anti-Stokes. The latter allows improvement in the reproduction of the DE dispersion.

To better understand the physical mechanisms involved, three fits are given in Fig. 3 for the following values of A_{eff}: (a) $A_{\text{eff}}=0.2\times10^{-6}$ erg cm^{-1}, i.e., largely underestimated with respect to its value for bulk cobalt and its best-fit value (see below); (b) $A_{\text{eff}}=0.5\times10^{-6}$ erg cm^{-1} (best-fit value); and (c) $A_{\text{eff}}=1.8\times10^{-6}$ erg cm^{-1} (bulk cobalt value[16]), thus considerably overestimating it with respect to the best fit. The major features of all three graphs can be explained by the peculiarities of the SW dispersion in the presence of the exchange (see Fig. 2). In the first case of a small exchange constant, the bulk spectrum becomes denser and the lowest BVSWs, giving the most significant optical contribution to the BLS line, are not at all resolved. They engender a single "collective" line separated from the DE peak in the anti-Stokes part of the spectrum. It appears symmetrically in the Stokes part. The DE Stokes response is not large and is barely visible. In the best-fit situation, the collective bulk response is more extended in the frequency domain due to a greater frequency spacing of individual SWR modes (see Fig. 2). The superposition of the two contributions leads to a characteristic "two-level" anti-Stokes line structure reproduced experimentally. Finally, in the last case of overestimated A_{eff} the DE and individual lines are well separated, with no overlapping taking place. Theory predicts a set of separate relatively narrow peaks. It should be added that this physically clear interpretation is based on rigorous magneto-optical simulations. Agreement between the theory and the experiment, for the best fit, is relatively good, considering the distortion at low frequencies of the measured BLS line by optical noise due to spurious elastic scattering.

The reduced value of A_{eff} can be explained, qualitatively, by the geometry of the nanocomposite structure, which is illustrated in Fig. 3(d). Although the theory of the tunneling-assisted interlayer exchange coupling has been developed simultaneously with that for more common metallic spacers,[17] there is much less experimental evidence confirming theoretical predictions. However, one can conclude that effective coupling can be achieved only when the dielectric spacer thickness is less than 1 nm,[18] which was confirmed in Ref. 11.

Exchange interactions between the particles are of point nature and the zones of effective tunneling do not cover all the "active" particle surface. The value of A_{eff} will drop off with the increase in the interparticle spacing. It will also decrease as a function of the particle size compared to the characteristic length of 1 nm since in this case the ratio of the actively interacting particle surface to its overall surface diminishes. Another important factor to be taken into account is the complex geometry, which can lead to even smaller values of A_{eff}.

Another question that arises, in a broader context, is the following: is the "superspin" approximation identifying a particle with a magnetic point with no internal structure adequate for the description of such a system? In the case of a simpler planar geometry of exchange-coupled magnetic stripes,[19] if the modes in individual stripes are in antiphase ($\Delta\varphi=\pi$), the function $\vec{m}(z)$ becomes discontinuous at the

interstripe interface. This is where the interlayer exchange comes in through the mixed Hoffman boundary conditions.[20] If intralayer A and interlayer A_{12} exchange constants are comparable, a non-negligible wave number is imposed on the dynamic magnetization within each layer. In other words, the distribution of $\vec{m}(z)$ becomes noticeably nonuniform. In Fig. 3(d) this variation in $\vec{m}(z)$ is indicated by corresponding variation in the color intensity. It is this internal inhomogeneity within each layer that pushes up the frequency of the coupled mode and this frequency shift is determined by the value of the intralayer A. Although in our case the interparticle phase mismatch is no longer necessarily equal to 0 or π, the major features are still present in the behavior of the system. More specifically, we would like to stress that it is finally through the inhomogeneity of the *internal dynamic magnetization* within each particle and *its internal exchange constant* that the dispersion of a magnetic nanocomposite film is shaped. In other words, the *superspin approximation*, regarding single-domain particles as a magnetic point with no internal structure, is no longer sufficient to adequately describe the high-frequency dynamics of a superferromagnetic film. It should be noted that the issue of the applicability of the superspin or macrospin model attracts more and more attention recently.[21]

To conclude, we have investigated, by means of the BLS technique, the behavior of the dipole-exchange magnetic excitations in a concentrated nanocomposite $Co_x(SiO_2)_{1-x}$ film ($x=80$ at. %) which is in the SFM state. Not surprisingly, the features typical of the presence of nonvanishing exchange interactions manifest themselves. The BVSW degeneracy is removed and the contributions the DE and backward volume modes can be identified in the Stokes and anti-Stokes BLS spectral lines. Numerical analysis of the fine structure of these lines allowed estimation of the value of the effective exchange constant A_{eff}. It turned out to be approximately three times less than that of its bulk value for the cobalt: $A=1.8\times10^{-6}$ erg cm^{-1}. Moreover, this analysis has indicated the presence of a relatively weak magnetic anisotropy on the order of several hundred oersteds.

To reliably identify the physical nature of the thermal magnons contributing to the BLS optical response, we performed our numerical simulations on two levels: magnetic and optical. The stochastic nature of the magnons is quantified via the FDT, while their dispersion characteristics were estimated by tensor magnetic Green's-function technique.

A qualitative theoretical model has been proposed to explain the reduction in the value A_{eff} with respect to A. It has been shown that the superspin approximation, identifying each nanoparticle with a magnetic point with no internal structure, is insufficient to account for the description of the SW behavior of a concentrated nanocomposite medium. The interparticle exchange interaction invariably leads to a pronounced redistribution of the dynamic magnetic field within each particle.

This work was supported by the French Ministry of National Education and Research (ACI NR0095 "NANODYNE") and Australian Research Council. A.V.Z. gratefully acknowledges financial support from EPSRC-GB.

*as@lpmtm.univ-paris13.fr

[1] S. Sankar, D. Dender, J. A. Borchers, D. J. Smith, R. W. Erwin, S. R. Kline, and A. E. Berkowits, J. Magn. Magn. Mater. **221**, 1 (2000).
[2] J. Inoue and S. Maekawa, Phys. Rev. B **53**, R11927 (1996).
[3] K. Yakushiji, S. Mitani, K. Takanashi, J.-G. Ha, and H. Fujimori, J. Magn. Magn. Mater. **212**, 75 (2000).
[4] J. S. Micha, B. Dieny, J. R. Régnard, J. F. Jacquot, and J. Sort, J. Magn. Magn. Mater. **272-276**, E967 (2004).
[5] W. F. Brown, Jr., Phys. Rev. **130**, 1677 (1963).
[6] J. Hesse, H. Bremers, O. Hupe, M. Veith, E. W. Fritscher, and K. Valtchev, J. Magn. Magn. Mater. **212**, 153 (2000).
[7] M. Azeggagh and H. Kachkachi, Phys. Rev. B **75**, 174410 (2007).
[8] T. Jonsson, P. Nordblad, and P. Svedlindh, Phys. Rev. B **57**, 497 (1998).
[9] P. E. Jönsson, S. Felton, P. Svedlindh, P. Nordblad, and M. F. Hansen, Phys. Rev. B **64**, 212402 (2001).
[10] X. Chen, S. Bedanta, O. Petracic, W. Kleemann, S. Sahoo, S. Cardoso, and P. P. Freitas, Phys. Rev. B **72**, 214436 (2005).
[11] S. Bedanta, T. Eimüller, W. Kleemann, J. Rhensius, F. Stromberg, E. Amaladass, S. Cardoso, and P. P. Freitas, Phys. Rev. Lett. **98**, 176601 (2007).
[12] A. Butera, J. N. Zhou, and J. A. Barnard, Phys. Rev. B **60**, 12270 (1999).
[13] J. Gómez, A. Butera, and J. A. Barnard, Phys. Rev. B **70**, 054428 (2004).
[14] A. I. Stognij, N. N. Novitskii, and O. M. Stukalov, Tech. Phys. Lett. **28**, 17 (2002).
[15] B. A. Kalinikos, N. V. Kozhus, M. P. Kostylev, and A. N. Slavin, J. Phys.: Condens. Matter **2**, 9861 (1990).
[16] Y. Roussigné, F. Ganot, C. Dugautier, P. Moch, and D. Renard, Phys. Rev. B **52**, 350 (1995).
[17] J. C. Slonczewski, Phys. Rev. B **39**, 6995 (1989).
[18] J. Faure-Vincent, C. Tiusan, C. Bellouard, E. Popova, M. Hehn, F. Montaigne, and A. Schuhl, Phys. Rev. Lett. **89**, 107206 (2002).
[19] M. P. Kostylev, A. A. Stashkevich, N. A. Sergeeva, and Y. Roussigné, J. Magn. Magn. Mater. **278**, 397 (2004).
[20] M. Vohl, J. Barnas, and P. Grünberg, Phys. Rev. B **39**, 12003 (1989).
[21] S. Rohart, V. Repain, A. Thiaville, and S. Rousset, Phys. Rev. B **76**, 104401 (2007).